Postnatal Development of the Skull of *Dinilysia patagonica* (Squamata-Stem Serpentes)

AGUSTÍN SCANFERLA[1]* AND BHART-ANJAN S. BHULLAR[2]

[1]CONICET, Instituto de Bio y Geociencias del NOA (IBIGEO), Museo de Ciencias Naturales de Salta, Salta, Argentina

[2]Department of Organismic and Evolutionary Biology, Harvard University, Cambridge, Massachusetts

ABSTRACT

The snake skull represents a profound transformation of the ancestral squamate cranium in which dermal skull roof bones were integrated with the braincase, in a manner convergent with that which occurred during the origin of mammals. However, the ontogeny of snake characters at the origin of the clade has until now been inaccessible. Here we describe a postnatal ontogenetic series of the Late Cretaceous stem snake *Dinilysia patagonica* and compare it to that of extant lizards and snakes. Comparative analysis indicates notable ontogenetic changes, including advanced state of ossification, isometric growth of the otic capsule, fusion of the stylohyal to the quadrate, and great posterior elongation of the supratemporal. Of these transformations, the unfused condition of braincase bones and the retention of a large otic capsule in adults are examples of paedomorphic and peramorphic processes, respectively. Some ontogenetic transformations detected, in particular those present in middle ear, skull roof and suspensorium, are strikingly similar to those present in extant snakes. Nevertheless, *Dinilysia* retains a lizard-like paroccipital process without an epiphyseal extremity, and a calcified epiphysis that caps the sphenoccipital tubercle. Finally, the integration of the dermal skull roof with the braincase is similar to that seen in mammals with regard to the overall closure of the braincase, but the two evolutionary and developmental modules appear less integrated in snakes in that the parietal bone of the dermal skull roof progressively overlaps the supraoccipital of the chondrocranial braincase. Anat Rec, 297:560–573, 2014. © 2014 Wiley Periodicals, Inc.

Key words: *Dinilysia*; postnatal ontogeny; extant snakes; heterochrony

INTRODUCTION

Fossil ontogenies are rich sources of new morphological and phylogenetic information regarding great transformations at the base of major vertebrate clades. Reptilian embryos and juveniles are a rarity in the fossil record, and the majority of those known are from nonavian dinosaurs (Delfino and Sánchez-Villagra, 2010). Up to now, no fossil snake ontogenies have been reported; thus, the only ontogenetic data available for snakes is from extant forms, although nearly all studies were focused on prenatal development. In fact, only three

previous studies describe the postnatal ontogeny of snakes, and all of these are largely concerned with quantitative analysis (Rossman, 1980; Young, 1989; Monteiro, 1998).

Dinilysia patagonica is considered one of the most important fossil squamates with respect to the discussion about snake origins, not only for its transitional phylogenetic position and morphology, but also for the large number of exquisitely preserved adult specimens recovered to date (Caldwell and Albino, 2002). In contrast with the traditional hypotheses that considers this fossil species as the sister taxon of Alethinophidia (Rieppel, 1979; Tchernov et al., 2000; Conrad, 2008; Wilson et al., 2010; Longrich et al., 2012), recent phylogenetic studies have proposed that *Dinilysia* represents the sister taxon to crown group Serpentes (Lee and Scanlon, 2002; Gauthier et al., 2012; Zaher and Scanferla, 2012). The importance of this fossil squamate has motivated several studies about its cranial morphology based on adult specimens (Estes et al., 1970; Frazzetta, 1970; Caldwell and Albino, 2002; Caldwell and Calvo, 2008; Zaher and Scanferla, 2012). Here, we provide novel information about skull anatomy of *Dinilysia* from an incomplete but informative postnatal ontogenetic sequence. The analysis of these specimens provides the first opportunity to study ontogenetic changes in the cranial anatomy of a transitional snake.

In light of our findings, we also discuss the integration of the cranial roof bones with the braincase elements to form a solid braincase, an anatomical acquisition that occurred in a convergent way to that of mammals. Study of this convergent evolutionary and developmental integration of the dermal skull roof with the chondrocranial braincase illuminates similarities and differences in the process between these hugely successful clades.

MATERIALS AND METHODS

Owing to the scarcity of published information about qualitative traits that change during postnatal development in snakes, we used ontogenetic sequences of representative taxa for each major clade of snakes (see Appendix). Juvenile individuals were the smallest individuals present in examined collections, although we cannot ascertain whether these prepared specimens are neonates or hatchling individuals. Information about embryonic development in snakes and lizards provided by the literature was also employed, in addition to CT scans of an embryo of the snake *Lampropeltis getula* and juveniles of some lizard species on the DigiMorph website (see Appendix).

The assembled ontogenetic sequence of *Dinilysia patagonica* comprises two small juvenile (Table 1) and eight large adult skulls. MLP 71-VII-29-1 is the smallest specimen, composed of a braincase that includes parietal (broken behind the postorbital constriction) supraoccipital, prootics, left supratemporal, incomplete left stapedial footplate, basioccipital, and the posterior region of the para-basisphenoid (Fig. 2A–D). Specimen MACN-N 106, more complete and slightly larger than MLP 71-VII-29-1, preserves the braincase (without stapes), quadrates, and posterior portion of both hemimandibles (Fig. 2E–H). All specimens of *Dinilysia* studied here were found in fluvial bedrocks corresponding to Bajo de la

TABLE 1. Cranial measurements of the postnatal ontogenetic sequence of *Dinilysia patagonica* (in mm)

	MLP 71-VII-29-1	MACN-N 106	MACN-RN 1014
Supraoccipital width	14,4	15,5	27,2
Supraoccipital length	5,3	4,9	6,1
Parietal width	12,8	13,8	33,1
Neurocranium width	18,8	20,4	44[a]
Quadrate length	X	7,8	17[a]
Supratemporal length	4,9	7,1	27,4
Paroccipital process length	0,2	1,3	6,8
Stapedial footplate length	6[a]	X	17,8

[a]Estimated.

Carpa Formation (Santonian, Upper Cretaceous) exposed in several localities distributed in Neuquén and Río Negro provinces, Argentina.

RESULTS

Taxonomic Identification

The small partial skulls MACN-N 106 and MLP 71-VII-29-1 exhibit several traits that provide useful information about their taxonomic attribution. These specimens bear a braincase wall laterally closed and otooccipitals that contact above the foramen magnum, both traits recognized as ophidian apomorphies (Rieppel, 1988; Cundall and Irish, 2008). Several features preserved in these specimens are also present in large skulls of *Dinilysia*, such as a distinctive I-shaped prootic and a sizeable fenestra ovalis. The presence of a ?-shaped quadrate, the paroccipital region formed by the paroccipital process of the otooccipital and the posterior region of the supratemporal, and the participation of the posterior process of the coronoid in the mandibular fossa, constitute characters that are also present in MACN-N 106 and adults of *Dinilysia*. MLP 71-VII-29-1 possesses a large stapedial footplate with small ridges originated at the base of the stapedial shaft, and posterolaterally projected crests on the ventral surface of the basisphenoid; these characters are also present in adult individuals of *Dinilysia*. Furthermore, other features present in these juvenile specimens (e.g. weak development of the crista prootica, anterior portion of the trigeminal foramen formed by the parietal) were also observed in juveniles of extant snakes. It is important to note that, as in analyzed ontogenetic sequences of extant snakes, transformation of these traits can be easily traced through the studied ontogenetic sequence of *Dinilysia*.

Considering this combination of shared characters, together with the same stratigraphic and geographic provenance, and the presence of several characters that represent transitional series, the small specimens studied here are herein assigned to *Dinilysia patagonica* Smith-Woodward, 1901. Additionally, given that Bajo de la Carpa Formation represents one of the best explored bedrock units of the Upper Cretaceous of NW Patagonia (Bonaparte, 1991; Leanza et al., 2004), the absence of other snake taxa reported from this sedimentary unit reinforces the taxonomic identification proposed here.

Morphological Changes in the Postnatal Series

The preserved cranial bones of juvenile specimens of *Dinilysia* are well-ossified, and there are no signs of fontanelles either in the roof or floor of the neurocranium. Nevertheless, in specimen MLP 71-VII-29-1 there is a small nonossified zone along the contact between basisphenoid, prootic and basioccipital (Fig. 2F). This condition is shared with most juvenile specimens of extant snakes examined, where there is an unossified area in this zone that is filled by cartilage and progressively ossifies in more advanced ontogenetic stages (Fig. 4C). This unossified zone is retained widely in adult specimens of scolecophidian snakes, an apparently paedomorphic condition (see List, 1966).

With the exception of exoccipital and opisthotic (see below), the rest of the components of the braincase in *Dinilysia* remain unfused as discrete elements during their postnatal lifespan as in most extant snakes, with the exception of some scolecophidians and uropeltids (Cundall and Irish, 2008). Another common characteristic among these juvenile specimens and juvenile squamates in general, is the bulbous shape of the braincase (Fig. 2A,E), a widespread feature of juvenile vertebrates (Emerson and Bramble, 1993). This characteristic juvenile shape changes during ontogeny, given that adult specimens exhibit a more rectangular configuration of the braincase due to the growth of the braincase bones, especially the components of skull roof, and the adductor chamber.

Parietal. This bone exhibits considerable caudal elongation, evidenced by the growth of the posterior border that overlaps the anterior region of supraoccipital (Fig. 3). Additionally, the supratemporal processes become larger in the posterolateral direction, in similar fashion to those of lizards (Maisano, 2001; Bhullar, 2012), *Anilius scytale*, and figured juvenile and adult specimens of *Cylindrophis ruffus* (Cundall and Irish, 2008: Fig. 2.35). In doing so, this process intercalates between the medial anterior margin of the supratemporal and the lateral region of the supraoccipital, and breaks the extensive contact between these bones observed in juvenile specimens. This posterior elongation results in the isolation of a small portion of the prootic that constitutes the only dorsal exposure of this bone in adult individuals. The postnatal transformation of the supratemporal process is strikingly similar to that in basal alethinophidians such as *Anilius* and *Cylindrophis*, which also display a small sliver of the prootic bone in the neurocranial roof. The sagittal crest, well developed in adults (Zaher and Scanferla, 2012) undoubtedly increases in size during postnatal ontogeny; however the timing of this enlargement is not possible to determine with precision in the juvenile specimens.

Supraoccipital. As was mentioned above, the supraoccipital undergoes a drastic reduction of its dorsal exposure owing to the roofing produced by the parietal posterior growth, especially in its lateral borders, which are covered by the growing supratemporal processes (Fig. 3). This pattern is similar to that observed in the *Anilius scytale* postnatal sequence and in *Cylindrophis ruffus* (Cundall and Irish, 2008: Fig. 2.35). In adult stages, the supraoccipital of *Dinilysia* exhibits strong sagittal and transverse crests (Fig. 3); these structures are incipiently developed in juvenile individuals. The transverse crest is also present in the basal alethinophidian *Cylindrophis*, and its development appears to occur during postnatal life also (see Cundall and Irish, 2008: Fig. 2.35). The otooccipitals are in contact dorsally to the foramen magnum, a feature also present in all postnatal stages of the extant snakes compared.

Otooccipital. This complex bone, formed by the fusion of the exoccipital and opisthotic (see Maisano, 2001), does not show traces of the fusion between these elements in either juvenile specimen. It is worth noting that a small portion of this suture does persist in examined juvenile specimens of *Typhlops brongersmianus* and *Boa constrictor*, a condition also observed in drawings of *Leptotyphlops humilis* (List, 1966: pl. 10-Fig. 6).

The paroccipital process, a characteristic feature of the opisthotic bone of reptiles, usually consists of an elongated, posterolaterally directed structure with a distal expanded tip capped by cartilage. During ontogeny, this process elongates and its cartilaginous extremity undergoes endochondral calcification and fuses with the distal tip in adults (Maisano, 2002a,b; Torres-Carvajal, 2003; Tarazona et al., 2008; Bhullar, 2012). A paroccipital process is present in adult specimens of *Dinilysia* (Estes et al., 1970; Zaher and Scanferla, 2012), and our observations of the ontogenetic sequence demonstrate that the genesis of this feature is the result of progressive elongation during postnatal development (Fig. 3). Despite a general resemblance to that of lizards, the paroccipital process of *Dinilysia* shows significant differences. In adults, the distal portion is formed by a tongue-like lamina, in contrast with the thick expanded quadrangular tip present in lizards. Additionally, there are no signs of suture of the calcified cartilage, and juveniles lack the porous surface that characterizes the distal tip of the paroccipital process of juvenile lizards. This distal porous surface represents the contact area with the growth plate of the paroccipital cartilaginous epiphysis. The lack of a recognizable calcified paroccipital epiphysis in adult specimens and the absence of a porous surface at the tip of the parocciptal process in juveniles indicate that the paroccipital epiphysis was not present in *Dinilysia*. Extant snakes such as *Anilius* show a still shorter paroccipital process than that of *Dinilysia*, and pythonid macrostomatans bear a small spike-shaped paroccipital process. Ontogenetic sequences of *Anilius scytale* and *Python sebae* demonstrate that this structure develops during postnatal life as in *Dinilysia* and lizards, and these snakes also lack the calcified cartilaginous extreme.

Prootic. As in adult ontogenetic stages, the shape of this bone in juvenile individuals is strongly influenced by the enormous size of the inner ear. As consequence of this condition, the prootic has a distinctly bulbous shape. Concomitantly, the sizeable fenestra ovalis occupies almost the entire prootic lateral wall. The crista circumfenestralis, an exclusive trait of the otic region of crown snakes and *Dinilysia* (see Zaher and Scanferla, 2012) surrounds the stapedial footplate and forms a pericapsular recess (Baird, 1970; Wever, 1978). The crista prootica, which is one of the components of the crista
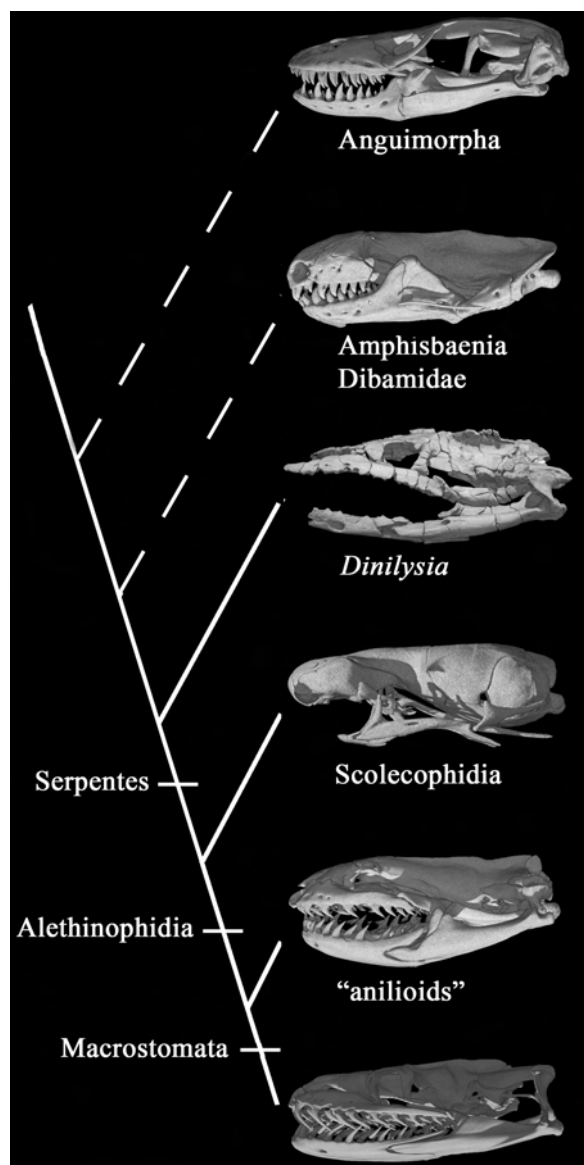
Fig. 1. Simplified phylogenetic tree of snakes showing amphisbaenian-dibamid and anguimorphs as alternative outgroups of crown Serpentes as was proposed by the most recent comprehensive analyses of squamate relationships.

circumfenestralis, forms a recess around the anterior part of the stapedial footplate in adult individuals of *Dinilysia* (Fig. 4D). Although the anterior part of the stapedial footplate is not present in specimen MLP 71-VII-29-1, it is possible to trace its anterior boundaries using the impression left by this structure in the sand matrix that fills the vestibular cavity. In this way, we ascertain that the stapedial footplate was not recessed in the prootic because of the weak development of the crista prootica in this juvenile stage (Fig. 4A). This configuration of the anterior part of the crista circumfenestralis coincides with that observed in juvenile extant snakes. The crista prootica (and crista circumfenestralis in general) exhibit a conspicuous growth during postnatal development such that extant snake species char-

acterized by a well-developed crista circumfenestralis in adult ontogenetic stages exhibit a poorly recessed stapedial footplate in juveniles (compare Fig. 4C,F).

In snakes, as in several burrowing lizards (e.g. amphisbaenians, dibamids, *Aniella*) and mammals, the descending lateral flange of the parietal encloses the braincase in the orbitotemporal region (Rieppel, 1989). In doing so, this flange contacts the anterior border of the prootic, including both dorsal and ventral anterior processes that surround the trigeminal foramen. During postnatal ontogeny, the anterior closure of the trigeminal foramen shows two conditions. Adult individuals of most extant snakes examined exhibit the trigeminal foramen formed by the prootic exclusively, due to the anterior growth of the processes (compare Fig. 4C,F). In some taxa, however, the processes cease or decrease their growth and do not come into contact, allowing the participation of the parietal bone in the trigeminal foramen (e.g. *Lichanura*).

Adult specimens of *Dinilysia* show the trigeminal foramen enclosed completely by the anterior processes of the prootic (Fig. 4E; Zaher and Scanferla, 2012). Nevertheless, the modest development of these process in the juvenile MLP 71-VII-29-1 allows the participation of the parietal bone in the trigeminal foramen in their anterior aspect (Fig. 4B). Thus, the complete closure of the trigeminal foramen by prootic bone occurred during postnatal development, a condition present in most extant snakes (Irish, 1989).

Stapes. The left stapedial footplate of the specimen MLP 71-VII-29-1 is positioned *in situ* and fitting the fenestra ovalis, although the proximal region is not preserved (Figs. 2G and 4A). The lateral surface of the footplate exhibits some pits and crests, as in adult specimens (Fig. 4D). A distinctive feature of the stapes of some basal group of snakes (scolecophidians, "anilioids", *Xenopeltis*) is the development of an articulation established between the otooccipital and an extensive concave area located in the posterodorsal corner of the stapedial footplate (Wever, 1978). This trait is also present in adult specimens of *Dinilysia* (Zaher and Scanferla, 2012) and in the juvenile specimen MLP 71-VII-29-1 (Fig. 4A), although in the latter it is expressed as a small lip developed in the posterodorsal corner of the footplate that is in close contact with the otooccipital.

Parabasisphenoid. Only the basisphenoid region of the specimen MLP 71-VII-29-1 is preserved, but some features such as the basipterygoid processes are not present (Fig. 2F). The preserved portion closely resembles the morphology of adult individuals. On the ventral surface, it is possible to distinguish two small crests originating in the posterior corners that run anterolaterally, a condition present in adult individuals that represents a plesiomorphic trait shared with lizards. As in the adult individuals, the basisphenoid exhibits a lateral expansion with a semicircular shape positioned at the base of the basipterygoid process.

Basioccipital. The sphenoccipital tubercles (=basal tubera) are ancestrally well-developed structures of the ventral braincase of squamates, which serve as the insertion of muscular ligaments from the cervical
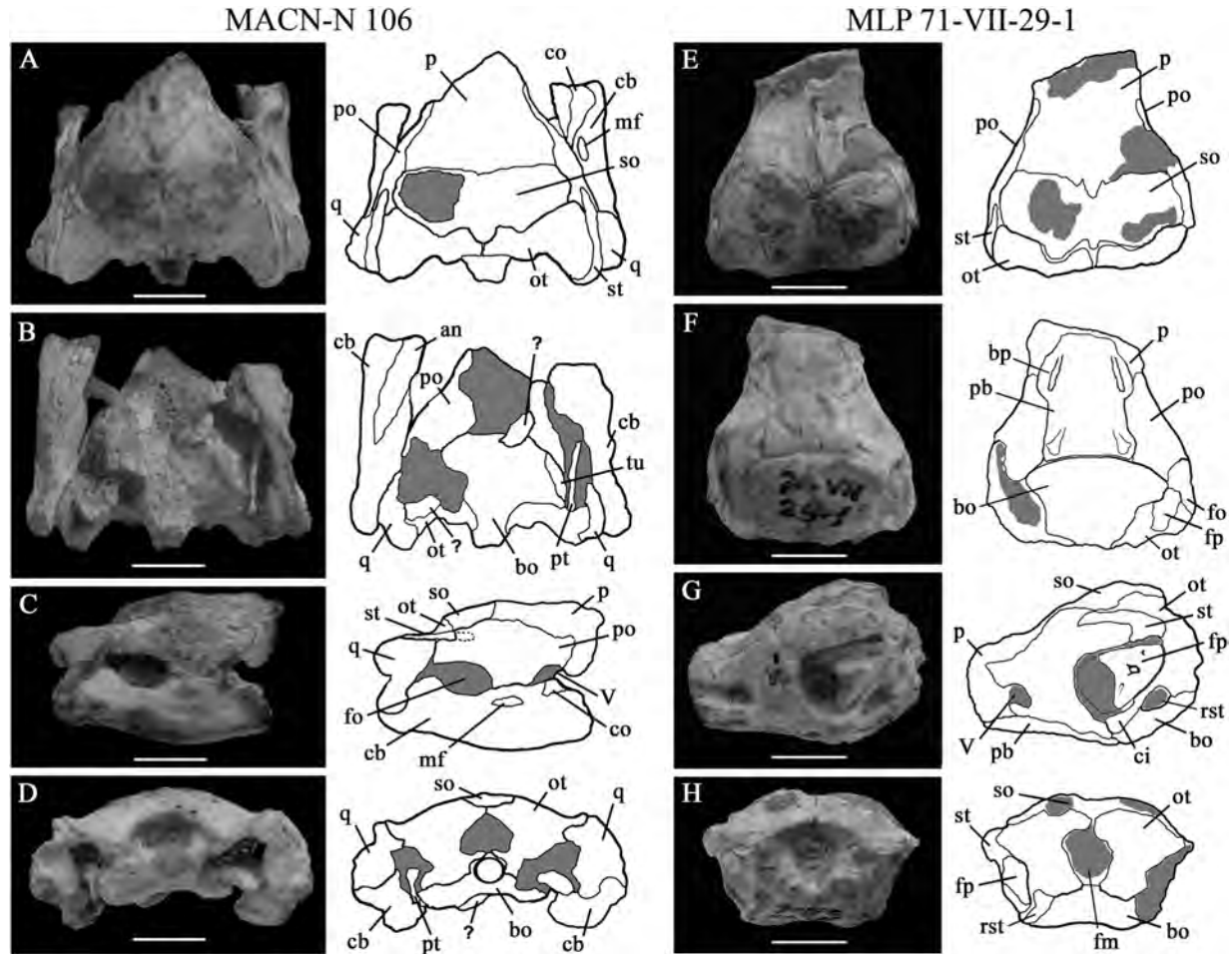
MACN-N 106

MLP 71-VII-29-1

Fig. 2. Juvenile specimens referred to *Dinilysia patagonica*, observed in dorsal (**A** and **E**), ventral (**B** and **F**), lateral (right **C**, left **G**), and posterior view. an, angular, bo, basioccipital, bp, base of the basipterygoid process, cb, compound bone, ci, crista interfenestralis, co, coronoid, fm, foramen magnum, fo, fenestra ovalis, fp, stapedial footplate, mf, mandibular fossa, ot, otooccipital, p, parietal, pb, parabasisphenoid, po, prootic, pt, pterygoid, q, quadrate, rst, recessus scalae tympani, so, supraoccipital, st, supratemporal, tu, sphenoccipital tubercle, V, trigeminal foramen. Scale bar equal to 5 mm.

musculature. Each tubercle consists of a lateroventral projection of the ventral surface of the basioccipital, and the distal tip is generally capped by a calcified cartilaginous epiphysis (Haines, 1969). Despite the widespread presence of this structure within lizards, there is little information in the literature about the postnatal ontogeny of this feature. The most detailed information about the postnatal trajectory of this trait comes from the description of the braincase of *Shinisaurus crocodilurus* published by Bever et al. (2005) and from the description of braincase ontogeny in the supplement of Bhullar (2012). In these lizards, the strong projection present in adult individuals is acquired progressively during postnatal ontogeny, and the calcification of the cartilaginous epiphysis does not occur until adult stages.

Adult specimens of *Dinilysia* exhibit well-developed sphenoccipital tubercles on the lateral region of the basioccipital (Fig. 5A,C), conferring a markedly concave shape to this bone in a similar fashion to that of lizards (Zaher and Scanferla, 2012). The development of this structure in the juvenile specimen MACN-N 106 is incipient (Fig. 2B), showing that the ventroposterior projec-

tion of this feature in adults is acquired progressively during postnatal life as in lizards. The adult specimen MACN-RN 1014 preserves details of the distal tip of the right sphenoccipital tubercle (Fig. 5A,B). Because of the lack of an epiphysis in this specimen, a porous texture is evident similar to that which characterizes the bony region located below the growth plate of the epiphysis in lizards (Fig. 5D). Of the numerous adult skulls recovered of *Dinilysia*, only MPCA-PV 527 preserves the epiphysis of the sphenoccipital tubercle (Fig. 5C); it can be characterized as an anteroposteriorly elongated structure that is applied over the almost surface of the tip of sphenoccipital tubercle as in lizards.

Supratemporal. The supratemporal increases in length considerably during postnatal development (Fig. 4). Anteriorly, the supratemporal grows between the prootic and the supratemporal process of the parietal. During postnatal life, the posterior region of the supratemporal follows the caudal elongation of the paroccipital process of the otooccipital, pushing the articular area
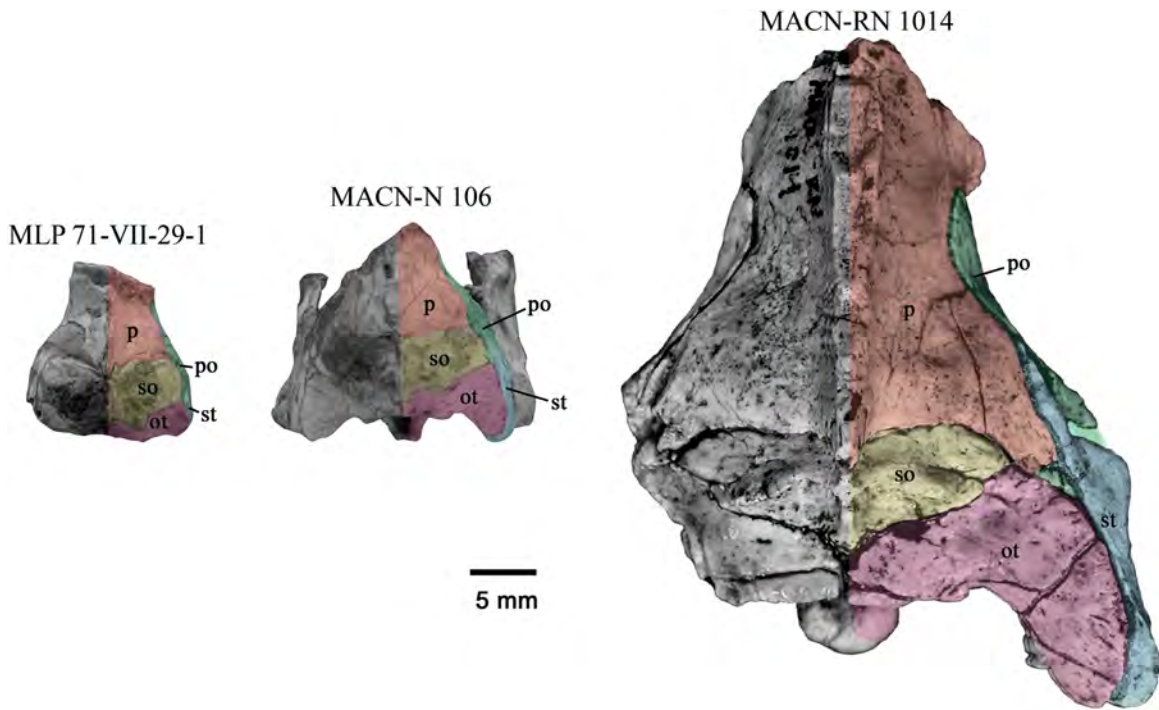
Fig. 3. Postnatal ontogenetic sequence of *Dinilysia patagonica* in dorsal view. Note the conspicuous enlargement of the posterolateral corner of the braincase (paroccipital process and supratemporal) and the progressive overlapping between skull roof elements.

with the quadrate bone well beyond the most posterior occipital border. This remarkable posterior growth contrasts with the condition exhibited by lizards, in which the supratemporal (and the paroccipital region in general) experiences a much lesser increase in length (Bhullar, 2012). The same caudal elongation is present in macrostomatan snakes, in which the supratemporal further acquires a free-ending process as a result of its posterior growth.

Quadrate. Both quadrates are preserved in juvenile specimen MACN-N 106. As in adults, this bone has a short and stout shape (Fig. 2C), a configuration shared with basal extant snakes such as typhlopids, "anilioids" and basal macrostomatans such as *Xenopeltis*. With increasing ontogenetic stage, this bone remains approximately the same proportional size, differing in its trajectory from the drastic longitudinal elongation observed in the quadrate of adult macrostomatans (Rossman, 1980; Young, 1989; Monteiro, 1999, personal observation).

In basal alethinophidians such as "anilioids" (*Anilius*, *Anomochilus*, and *Cylindrophis*) and the basal macrostomatan *Xenopeltis*, the stylohyal consists of a somewhat spherical structure fused at the posteromedial region of the quadrate suprastapedial process (Fig. 6D). The distinct nature of the stylohyal with respect to the rest of the quadrate bone can be easily determined in CT scan images (moth-eaten appearance) as well as dry skeletons (granular appearance) of these snake species, because their particular surface texture clearly differs with the smooth surface exhibited by the rest of the quadrate.

Additionally, it is possible to distinguish the boundaries of the fused stylohyal because a shallow groove persists between it and the quadrate suprastapedial process. Adult individuals of *Dinilysia* exhibit a well-developed suprastapedial process as in "anilioids" and *Xenopeltis*. The distal region of this process, well-preserved in adult specimens MACN-RN 1013 (Fig. 6B) and MACN-RN 1014 (Fig. 6C), is applied against the ventral portion of the supratemporal posterior tip. Detailed observation of this area reveals that this portion contains a somewhat spherical portion distinguishable from the rest of the suprastapedial process. Additionally, this structure can be easily recognized through direct observation by its granular surface, whereas a "moth-eaten" texture helps to distinguish this structure in CT scan images (Fig. 6B). In juvenile MACN-N 106 the left and right quadrate exhibit different preservations in the posterior region of the cephalic condyle (Fig. 6A). The right quadrate exhibits a spherical structure applied to the posteromedial area of the suprastapedial process, which is also in contact with the posterior tip of the supratemporal as in adult specimens. Its surface has a granular texture, in contrast to the smooth solid surface of the rest of surrounding bones. This structure is not preserved completely in left quadrate, allowing the observation of the posterior part of the suprastapedial process. The latter region exhibits a well-delimited surface that is in contact with a small fragment corresponding to the spherical structure completely preserved in the right quadrate (Fig. 6A).

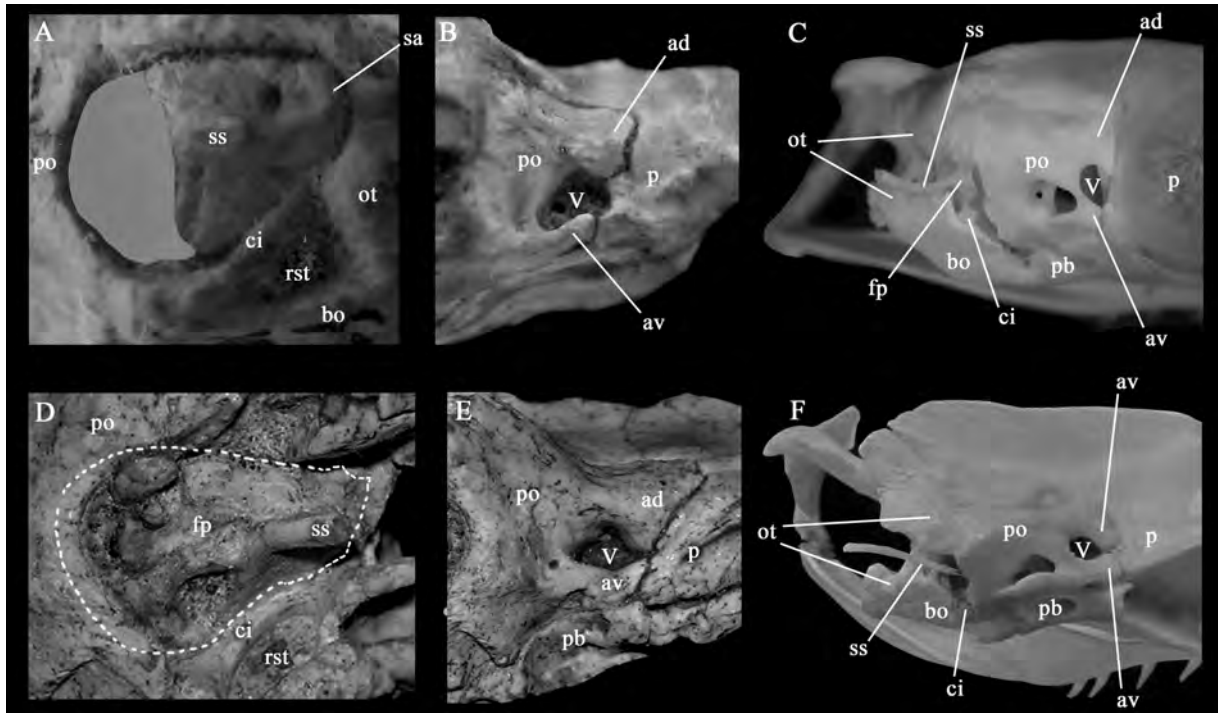The morphology and topological relationships of the spherical structure fused to the posterior region of the

Fig. 4. Notable anatomical changes in braincase of *Dinilysia pata-gonica*. Left stapedial footplate and surrounding area of juvenile specimen MLP 71-VII-29-1 (**A**) and adult specimen MACN-RN 1014; Lateral view of right trigeminal foramen of juvenile specimen MLP 71-VII-29-1 (**B**) and adult specimen MACN-RN 1014 (**E**); Posterolateral view of the braincase of juvenile (**C**) and adult (**F**) specimens of the extant macrostomatan snake *Boa constrictor*. ad, anterior dorsal process, av, anterior ventral process, ci, crista interfenestralis, fp, stapedial footplate, po, prootic, rst, recessus scalae tympani, sa, stapedial articulatory surface, ss, stapedial shaft, V, trigeminal foramen.

suprastapedial process of juvenile and adult specimens of *Dinilysia* is strikingly similar to that of the stylohyal present in "anilioids" and *Xenopeltis* (compare Fig. 6B,D). Moreover, the relation established between this structure and the stapedial shaft in adult specimen MACN-RN 1,014 strongly resembles that observed in *Xenopeltis*, where an intermediary element is interposed between the stapedial shaft and the fused stylohyal in both taxa (Frazzetta, 1999; Caldwell and Albino, 2002; Zaher and Scanferla, 2012). Hence, we propose that the spherical structure fused to the suprastapedial process of the quadrate of juvenile and adult specimens of *Dinilysia* actually represents the ophidian stylohyal.

Lower jaw. Specimen MACN-N 106 preserves the posterior portion of both mandibles (Fig. 1B), although only the right jaw is satisfactorily preserved. Lower jaw morphology shows little change during postnatal ontogeny, with the exception of the elongation of the postdentary region of the compound bone. Concomitantly, the prearticular crest of the compound bone experiences an elongation towards the articular region (Fig. 2C).

DISCUSSION

State of Ossification and Fusion of the Braincase Elements

As in juvenile extant snakes, both MLP 71-VII-29-1 and MACN-N 106 display complete ossification of skull roof and absence of broad unossified zones in the basi-

cranium. However, it must be emphasized that these juvenile specimens are not hatchling/neonate individuals, and the possibility that perinates of *Dinilysia* could have had some unossified zones cannot be ruled out. The advanced state of ossification observed in juvenile snakes is in concordance with the precocial developmental condition present in cranial bones of late embryos (Brock, 1929; Kamal and Hammouda, 1965; Genest-Villard, 1966; Kamal et al., 1970; Haluska and Alberch, 1989; Rieppel and Zaher, 2001; Jackson, 2002; Boughner et al., 2007; Polachowsky and Werneburg, 2013), suggesting that accelerated maturity of the head skeleton since perinatal stages is an apomorphic trend shared by *Dinilysia* and extant snakes.

The above-mentioned condition present in *Dinilysia* and snakes is in contrast with juveniles of most lizard groups, which exhibit less skeletal maturity (Maisano, 2001). Notably, amphisbaenians are an exception among lizards because these snake-like lizards have closed braincase in a similar manner to snakes. Although there is little information about the embryonic and postnatal development in this fossorial serpentiform group, the available data indicate that skull roof elements and chondrocranial elements of the neurocranium are fully ossified and fused in late embryos and/or juvenile postnatal individuals (Kritzinger, 1946; Montero et al., 1999; Maisano, 2001; personal observation).

Despite the early state of ossification described above, endochondral constituents of the braincase of *Dinilysia* remain unfused as discrete bones throughout postnatal life, with the sole exception of the complete fusion
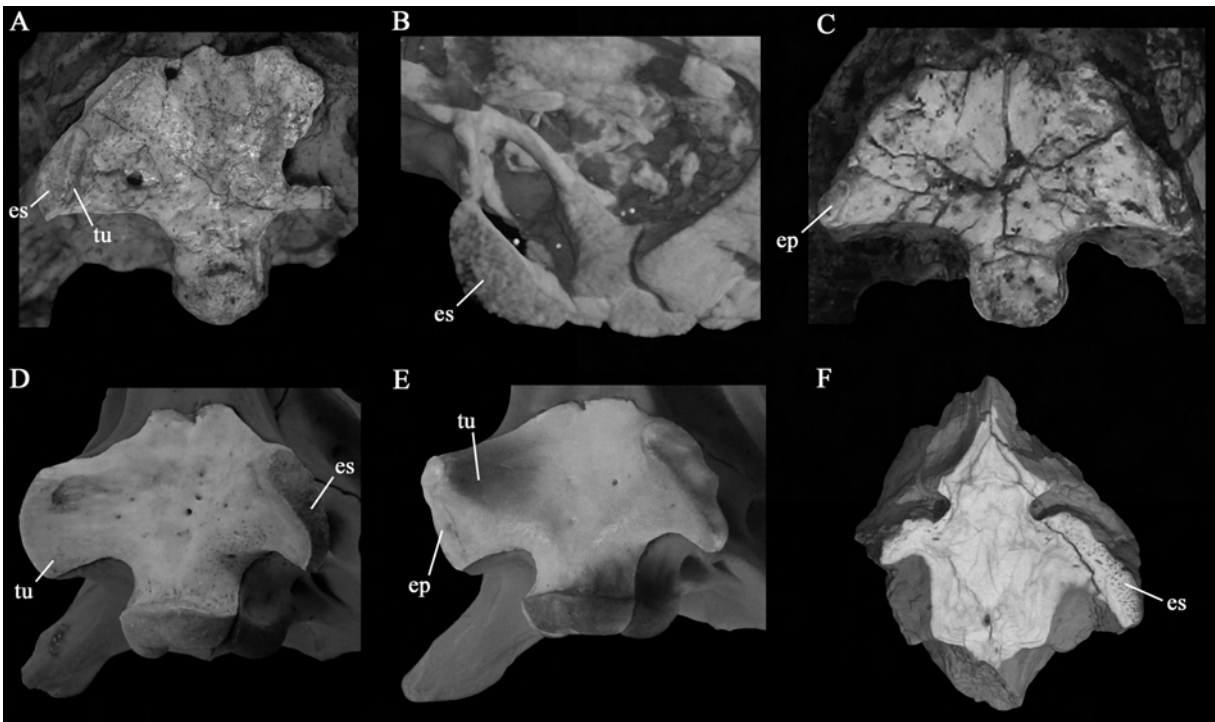
Fig. 5. The sphenoccipital tubercle anatomy of *Dinilysia patagonica*. Ventral view of the basioccipital of the specimen MACN-RN 1014 (**A**), and lateral view of three-dimensional reconstruction based on HRXCT data of the same specimen (**B**) showing the porous structure of the tip of sphenoccipital tubercle; **C**, ventral view of the basioccipital of the specimen MPCA-PV 527; ventrolateral view of the basioccipital of a subadult (**D**) and adult (**E**) specimens of the teiid lizard *Tupinambis merianae*; **F**, three-dimensional cutaway view along the frontal axis of preserved braincase fragment of the malagasy cretaceous snake *Menarana nosimena*. sphenoccipital tubercle. ep, epiphysis of the sphenoccipital tubercle, es, epiphysial surface contact, tu, sphenoccipital tubercle.

between exoccipital and opisthotic. Although some scolecophidian species (List, 1966; Cundall and Irish, 2008) and most uropeltids (Rieppel and Zaher, 2002; Olori and Bell, 2012) are exceptions, endochondral braincase bones of most adult snakes remain unfused as in *Dinilysia*. A few colubroids display some degree of fusion between braincase bones in late adult specimens, but this fusion may represent a superficial overgrowth of the involved sutures (Laduke et al., 2010a). Taking into account that most studied lizard species exhibit fusion of the braincase elements in adult individuals (Maisano, 2001; Bever et al., 2005; Tarazona et al., 2008), the apomorphic condition of unfused braincase in adults shared by *Dinilysia* and most extant snakes is interpreted as paedomorphosis due to a low rate of replacement of synchondrosis by synostosis.

Otic Capsule

During the development of tetrapod vertebrates, the early differentiation and growth of the central nervous system and sensory capsules yields embryos and neonates with large braincases, eyes and auditory regions relative to the rest of the skull (Emerson and Bramble, 1993). In consequence, postnatal development generates a relative reduction of the braincase and sensory capsules coupled with proportional enlargement of the facial region (i.e. negative allometry). This pattern is present in most squamates with respect to the otic capsule (e.g.

Bhullar, 2012), where a small otic region diminishes relatively their size during postnatal ontogeny (Fig. 7B). However, the size of the otic capsule observed along the studied postnatal sequence of *Dinilysia* suggests a strikingly different ontogenetic trajectory. Although the preservation of specimens precludes an exhaustive metric analysis, comparisons of the otic region at same braincase length between juvenile and adult stages (Fig. 7A) suggest that stapes (and consequently otic capsule) grew following an isometric trajectory during postnatal ontogeny, in clear contrast with the typical negative allometry followed by the components of the otic region in most squamates. The consequence of this isometry is the apomorphic retention of an enormous otic region in adult specimens of *Dinilysia* (Fig. 7C). Large otic capsules are a characteristic trait of adult individuals of miniaturized burrowing lizards (Rieppel, 1984) and scolecophidian snakes. However, it is important to note that all of these forms possess a small body size (generally no more than 30–40 cm), whereas regression analyses suggest that *Dinilysia* reached 2 meters in length (Scanferla, 2010). A possible explanation of this unusual feature is that the otic region of *Dinilysia* experiences during its postnatal ontogeny an extension of the growth curve with respect to the ancestral condition (i.e. peramorphosis) reflecting by a miniaturized (probably fossorial) squamate ancestor with large otic capsules. This hypothesis evokes and supports the evolutionary scenario for the origin of snakes conceived by Rieppel (1984), who
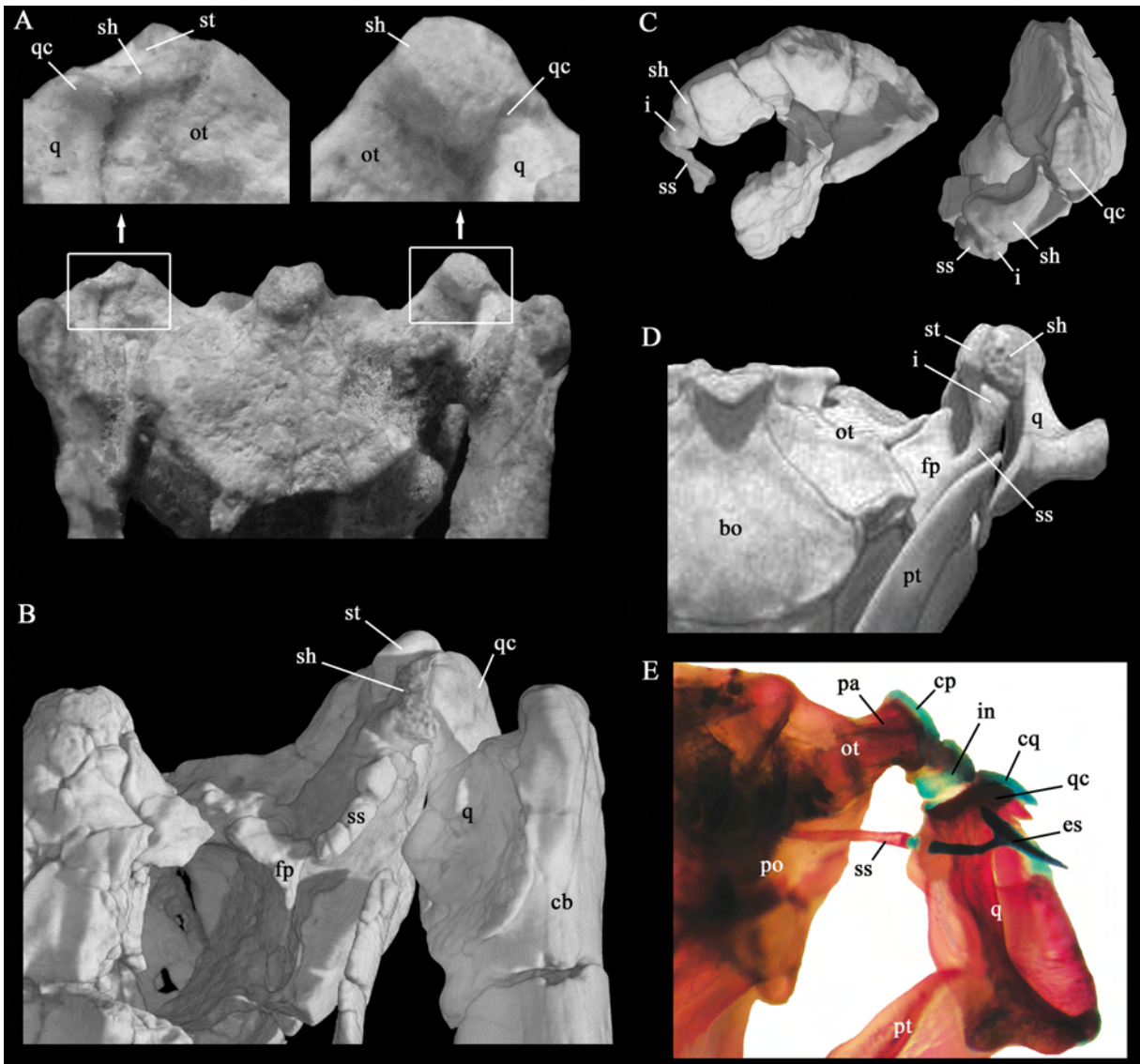
Fig. 6. Middle ear structure in *Dinilysia patagonica*. **A**, Ventral view of juvenile specimen MACN-N 106 with details of the suspensorium; **B**, three-dimensional reconstruction based on HRXCT data of adult specimen MACN-RN 1013 in ventral view; **C**, three-dimensional reconstruction based on HRXCT data of right quadrate of adult specimen MACN-RN 1014 in lateroventral (left) and posterodorsal (right) view; **D**, right ventral view of three-dimensional reconstruction based on HRXCT data of braincase of *Xenopeltis unicolor*; **E**, posteroventral view of a cleared and stained skull of the iguanian lizard *Liolaemus albiceps*, showing the cartilages and bones involucrated in the suspensorium. Note the mineralization of the intercalary cartilage evidenced by the mixed red (alizarin) and blue (alcian) staining. cb, compound bone, cp, cartilage capping the paroccipital process, cq, cartilage capping quadrate cephalic condyle, es, extrastapes, fp, stapedial footplate, i, intermediary ossification between stapes and stylohyal, in, intercalary, ot, otooccipital, pa, paroccipital process, po, prootic, pt, pterygoid, q, quadrate, qc, quadrate cephalic condyle, sh, stylohyal, ss, stapedial shaft, st, supratemporal.

proposed that some traits gained by a burrowing miniaturized ancestor of snakes were retained during the return to a surface habitats and subsequent body size increase. In this way, the above mentioned advanced state of ossification observed in perinate individuals of extant snakes and juveniles of *Dinilysia* could represent another trait inherited from fossorial ancestors that perdured in the ophidian lineage. The persistence of these traits in snakes appears to be an example of phylogenetic inertia (see Blomberg and Garland [2002] for more precision about this evolutionary process) after the cessation of the selective forces that imposes the burrowing behavior.

Middle Ear

The middle ear of snakes is distinctive among squamates owing to the particular contact between the distal tip of the stapedial shaft with the stylohyal, which is fused to the quadrate bone. The stylohyal is a homologue of the intercalary cartilage of nonophidian squamates (Rieppel, 1980), which is generally involved in the
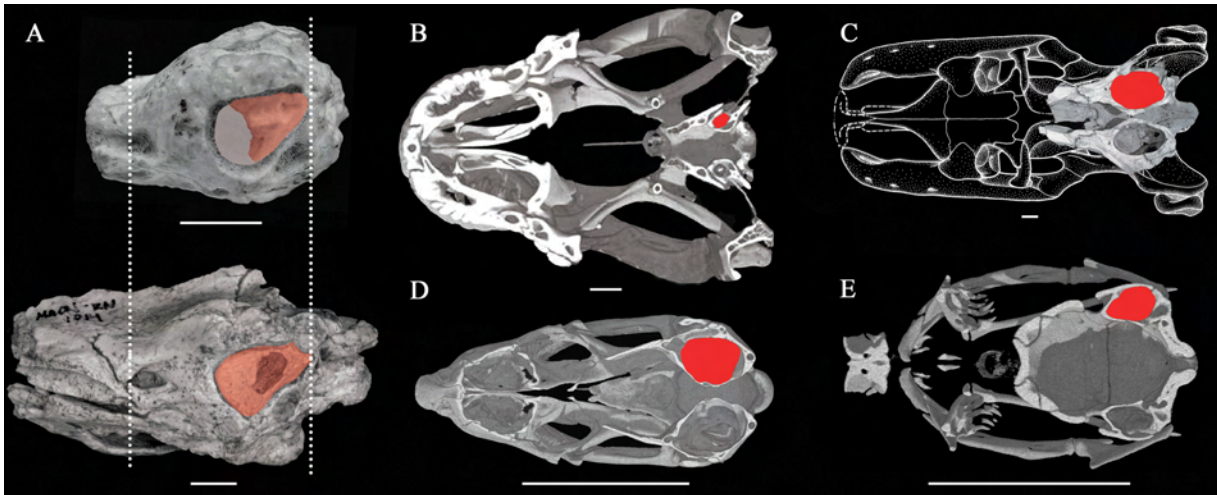
Fig. 7. **A**, Juvenile (top) and adult (bottom) of *Dinilysia patagonica* figured to the same prootic length (=anterior edge of the trigeminal foramen to posterior edge of fenestra ovalis). This plate reveals isometry of the otic region, expressed externally through fenestra ovalis and stapedial footplate. Three-dimensional cutaway views along the frontal plane of *Heloderma suspectum* (**B**), *Dinilysia patagonica* (**C**), *Aniella pulchra* (**D**), and *Typhlops jamaicensis* (**E**) based on HRXCT data. All complete skulls have been figured to the same skull length. Reconstruction of *Dinilysia* skull follows Zaher and Scanferla (2012). Scale bar equal to 5 mm.

suspension of the quadrate bone in lizards (Oelrich, 1956). In his work on middle ear anatomy in snakes, Rieppel (1980) established two conditions in the fusion of the stylohyal to the quadrate bone: in basal alethinophidians ("anilioids") and some basal macrostomatans (e.g. *Xenopeltis*) this structure fuses with the posterior tip of the suprastapedial process, whereas in most macrostomatan snakes that lack a defined suprastapedial process it fuses with the quadrate shaft.

Caldwell and Albino (2002) were the first to distinguish an intermediary element between the stapedial shaft and the quadrate in an adult specimen of *Dinilysia* (MACN-RN 1014). These authors identified this structure as the "… *extracolumella/intercalary/stylohyal element that articulates with the suprastapedial process of the quadrate*," but shortly after in the same paper referred to it as the stylohyal (Caldwell and Albino, 2002; p 865). It is worth noting that this structure does not correspond with the stylohyal recognized here. There exist other snakes with one or more intermediary elements between the stapedial shaft and the stylohyal (named as "intervening cartilages" by Wever [1978]), but the homology of these is not as of yet possible to determine. The evidence presented here indicate that the stylohyal in *Dinilysia* is fused with the suprastapedial process as in "anilioids" and the basal macrostomatan *Xenopeltis*, and that the ball-shaped element described by Caldwell and Albino (2002) results an intermediary structure similar to that present in *Xenopeltis* (Frazzetta, 1999) and other snakes (Wever, 1978).

The particular texture that denotes the stylohyal of *Dinilysia* and basal snakes such as "anilioids" and *Xenopeltis* may indicate an important degree of endochondral calcification that characterizes the stylohyal as a cartilaginous tissue (see Maisano, 2002b), a process that occurs through deposition of granular organic-inorganic particles in the cartilage matrix (Bonucci and Gómez, 2012). Although a histological study is necessary to confirm the nature of the stylohyal in *Dinilysia* and snakes,

the homology of this structure with the intercalary cartilage of nonophidian lizards can be invoked as another line of evidence that supports this inference. Personal observations carried out in cleared and stained lizard specimens reveal that this cartilage undergoes calcification during postnatal ontogeny (Fig. 6E). This observation supports the postnatal ontogenetic trajectory of the stylohyal of *Dinilysia* and most extant snakes as a calcified endochondral cartilage that become fused to the quadrate. Thus, the presence of typical snake middle ear morphology in *Dinilysia* demonstrates that the recruitment of the stylohyal (=intercalary) as an element of the middle ear system and their postnatal ontogenetic trajectory was present early in the history of snakes.

Suspensorium

Estes et al. (1970) were the first authors to note the remarkable posterior extension of the supratemporal bone in *Dinilysia*. Our ontogenetic analysis indicates that this extension, together with the concomitant elongation of the paroccipital process of the otooccipital, took place during postnatal life. This ontogenetic trajectory resembles the caudal elongation experienced by supratemporal during postnatal development in macrostomatans (Rossman, 1980; Young, 1989; Rieppel, 1993; Monteiro, 1999; personal observation), which generates the free-ending process responsible for the characteristic posterior position of the suspensorium in this group of alethinophidians. The posterior extension of the suspensorium allows the mandibular elongation, which together with potential deformation (i.e. intramandibular joint) and the potential separation of the mandibles constitute the main requisites to enlarge the cross-sectional area of the mouth in snakes (Arnold, 1983; Cundall and Greene, 2000). Remarkably, *Dinilysia* displays a considerable mandibular elongation enabled by the increasing posterior growth during postnatal development of the supratemporal, and a well-developed

intramandibular joint (Caldwell and Calvo, 2010; Zaher and Scanferla, 2012). Notwithstanding, caution should be taken with the degree of macrostomy that could have been displayed by *Dinilysia*, because the capability to swallow whole large prey depends on several anatomical features that are hardly possible to recognize in fossil species (Cundall and Greene, 2000; Cundall and Irish, 2008).

If the hypothesized position of *Dinilysia* as stem snake is accurate, then these traits necessary for macrostomy were present early in snake evolution. Furthermore, this hypothesis indicates that extant basal snakes such as scolecophidians and "anilioids" suffered a notable reversion of these features, a condition labeled by Rieppel (2012) as "regressed macrostomatan." Although we agree with Rieppel's (2012) arguments against the idea of basal snakes as regressed macrostomatans, the position of *Dinilysia* as stem snake suggest that fossorial basal snakes have lost some osteological characters necessary for macrostomy, regardless of the position of marine symoliophiids in the snake tree.

Sphenoccipital Tubercle

In addition to *Dinilysia*, the fossil snakes *Wonambi* (Scanlon, 2005), *Yurlunggur* (Scanlon, 2006), and *Menarana nosymena* (Laduke et al., 2010a) also bear well-developed sphenoccipital tubercles, although the specimens available of these taxa did not preserve the sphenoccipital epiphysis. Of the numerous recovered skulls of *Dinilysia*, only the right sphenoccipital tubercle of the specimen MPCA 527 retains its epiphysis and thus represents the first record of this structure in a snake. The lack of preservation of epiphysis in juvenile and most adult individuals seems to indicate a latter fusion of this structure with respect to extant lizards examined. Furthermore, the presence of a porous surface at the tip of the sphenoccipital tubercle that supported a growth plate suggests that the sphenoccipital tubercle in *Dinilysia* had a similar ontogenetic trajectory to lizards. However, a close observation of the available horizontal cutaway CT scan data of *Menarana* (Laduke et al., 2010b; Fig. 5F) reveals that the tip of the left sphenoccipital tubercle exhibit the same porous morphology as the epiphyseal area of *Dinilysia*. This shared characteristic suggests the possibility that the sphenoccipital tubercle of *Menarana* was also capped by an epiphysis, and also indicates that a lizard-like sphenoccipital tubercle was a widespread trait in Cretaceous snakes.

Previous authors have pointed out the absence of axial epiphyses as a distinct feature of snakes (Haines, 1969; Rieppel, 1988). However, in addition to the reported existence of epiphysis in the sphenoccipital tubercle of *Dinilysia* and probably *Menarana*, Kley (2006) described a proximal epiphysis in the quadrate bone of the scolecophidian *Rena dulcis*. Therefore, thorough ontogenetic scrutiny of extant species is necessary to establish the presence of epiphyseal centers in the axial skeleton of snakes.

Integration of Dermal Roof Elements and Braincase in Convergent Occurrences of Closed Crania

Mammals and snakes show perhaps the most extensive closure of the skull surrounding the brain among vertebrates (Rieppel, 1989). In general, the closure of the snake cranial wall resembles that seen in plesiomorphic mammaliaforms (Kermack et al., 1981). In mammals, the dermal cranial roof is confluent and deeply integrated with the braincase. For instance, in the ontogenetic sequence of the conservative therian *Monodelphis domestica* on the DigiMorph website (www.digimorph.org), it is evident that the parietal-supraoccipital suture is fixed and the interparietal ossifies over the top of the supraoccipital. In *Dinilysia* and several snakes, on the other hand, the parietal grows backward to overlap and cover over most of the supraoccipital. Thus, in snakes, the dermal cranial roof appears to be more modular and less integrated with the chondrocranial braincase than in the convergent mammalian situation.

LITERATURE CITED

Arnold SJ. 1983. Morphology, performance and fitness. Am Zool 23: 347–361.

Baird IL. 1970. The anatomy of the reptilian ear. In: Gans C, Parsons TS, editors. Biology of the reptilia. Vol. 2: Morphology B. London: Academic Press. p 193–275.

Bever GS, Bell CJ, Maisano JA. 2005. The ossified braincase and cephalic osteoderms of *Shinisaurus crocodilurus* (Squamata, Shinisauridae). Palaeontol Electron 8:1–36.

Bhullar B-AS. 2012. A phylogenetic approach to ontogeny and heterochrony in the fossil record: cranial evolution and development in anguimorphan lizards (reptilia: squamata). J Exp Zool Part B 318:521–530.

Blomberg SP, Garland T. 2002. Tempo and mode in evolution: phylogenetic inertia, adaptation, and comparative methods. J Evol Biol 15:899–910.

Bonaparte JF. 1991. Los vertebrados fósiles de la Formación Rio Colorado, de la ciudad de Neuquén y cercanías, Cretácico Superior, Argentina. Rev Mus Arg Cs Nat 4:16–123.

Bonucci E, Gomez S. 2012. Cartilage calcification. In: Seto J, editor. Advanced topics in biomineralization. InTech, Available at: http://www.intechopen.com/books/advanced-topics-in-biomineralization/cartilage-calcification. Accessed November 12, 2012.

Boughner JC, Buchtova M, Fu K, Diewert VW, Hallgrímsson B, Richman JM. 2007. Embryonic development of *Python sebae*. I: staging criteria and macroscopic skeletal morphogenesis of the head and limbs. Zoology 110:212–230.

Brock GT. 1929. On the development of the skull of Leptodeira hotamboia. Q J Microsc Sci 73:289–334.

Caldwell MW, Albino AM. 2002. Exceptionally preserved skeletons of the Cretaceous snake *Dinilysia patagonica* Woodward, 1901. J Vert Paleontol 22:861–866.

Caldwell MW, Calvo J. 2008. Details of a new skull and articulated cervical column of *Dinilysia patagonica* Woodward, 1901. J Vert Paleontol 28:349–362.

Conrad JL. 2008. Phylogeny and systematics of Squamata (Reptilia) based on morphology. Bull Amer Mus Nat Hist 310:1–183.

Cundall D, Greene HW. 2000. Feeding in snakes. In: Schwenk K, editor. Feeding: form, function and evolution in tetrapod vertebrates. San Diego: Academic Press. p 293–333.

Cundall DF, Irish F. 2008. The snake skull. In: Gans C, Gaunt AS, Adler K, editors. Biology of the reptilia, Vol. 20: Morphology H, The Skull of Lepidosauria. Ithaca, NY: Society for the Study of Amphibians and Reptiles. p 349–692.

Delfino M, Sánchez-Villagra MR. 2010. A survey of the rock record of reptilian ontogeny. Semin Cell Dev Biol 21:432–440.

Emerson SB, Bramble DM. 1993. Scaling, allometry, and skull design. In: Hanken J, Hall BK, editors. The skull. Vol. 3: Functional and evolutionary mechanisms. Chicago: University of Chicago Press. p 384–416.

Estes R, Frazzetta TH, Williams EE. 1970. Studies on the fossil snake *Dinilysia patagonica* Woodward: Part 1. Cranial morphology. Bull Mus Comp Zool 140:25–74.

Frazzetta TH. 1970. Studies on the fossil snake *Dinilysia patagonica* Woodward. Part II. Jaw machinery in the earliest snakes. Forma et Functio 3:205–221.

Frazzetta TH. 1999. Adaptations and significance of the cranial feeding apparatus of the sunbeam snake (*Xenopeltis unicolor*): Part I. Anatomy of the skull. J Morphol 239:27–43.

Gauthier JA, Kearney M, Maisano JA, Rieppel O, ADB Behlke. 2012. Assembling the Squamate tree of life: perspectives from the phenotype and the fossil record. Bull Peabody Mus Nat Hist 53: 1–308.

Genest-Villard H. 1966. Développement du crâne d'un boidé: *Sanzinia madagascariensis*. Mém Mus Natl Hist Nat A 40:207–262.

Haines RW. 1969. Epiphyses and sesamoids. In: C Gans, Bellairs A, Parsons TS, editors. Biology of the Reptilia, Vol. 1 Morphology A. London: Academic Press. p 81–122.

Haluska F, Alberch P. 1989. The cranial development of *Elaphe obsoleta* (Ophidia, Colubridae). J Morphol 178:37–55.

Irish FJ. 1989. The role of heterochrony in the origin of a novel bauplan: evolution of the ophidian skull. Géobios Mém Spec 12: 227–233.

Jackson K. 2002. Post-ovipositional development of the monocled cobra, *Naja kaouthia* (Serpentes: Elapidae). Zoology 105:203–214.

Kamal AM, Hammouda HG. 1965. The development of the skull of *Psammophis sibilans* III: the osteocranium of a late embryo. J Morphol 116:297–310.

Kamal AM, Hammouda HG, Mokhtar FM. 1970. The development of the osteocranium of the Egyptian cobra I: the embryonic osteocranium. Acta Zool 1970: 1–17.

Kermack KA, Mussett F, Rigney HW. 1981. The skull of *Morganucodon*. Zool J Linn Soc 71:1–158.

Kley NJ. 2006. Morphology of the lower jaw and suspensorium in the Texas blindsnake, *Leptotyphlops dulcis* (Scolecophidia: Leptotyphlopidae). J Morphol 267:494–515.

Kritzinger CC. 1946. The cranial anatomy and kinesis of the South African amphisbaenid *Monopeltis capensis* Smith. S Afr J Sci 42: 175–204.

Laduke TC, Krause DW, Scanlon JD, Kley NJ. 2010a. A late Cretaceous (Maastrichtian) snake assemblage from the Maevarano formation, Mahajanga Basin, Madagascar. J Vert Paleontol 30:109–138.

Laduke TC, Krause DW, Scanlon JD, Kley NJ. 2010b. "*Menarana nosymena*" Available at http://digimorph.org/specimens/Menarana_nosymena/. Accessed January 15, 2013.

Leanza HA, Apesteguía S, Novas FE, de la Fuente M. 2004. Cretaceous terrestrial beds from the Neuquén Basin (Argentina) and their tetrapod assemblages. Cret Res 25:61–87.

Lee MSY, Scanlon JD. 2002. Snake phylogeny based on osteology, soft anatomy and ecology. Biol Rev 77:333–401.

List JC. 1966. Comparative osteology of the snake families Typhlopidae and Leptotyphlopidae. Illinois Biol Monog 36:1–112.

Longrich NR, Bhullar BAS, Gauthier JA. 2012. A transitional snake from the Late Cretaceous period of North America. Nature 488: 205–208.

Maisano JA. 2001. A survey of the state of ossification in neonatal squamates. Herpetol Monog 15:135–157.

Maisano JA. 2002a. Postnatal skeletal ontogeny in *Callisaurus draconoides* and *Uta stansburiana* (Iguania: Phrynosomatidae). J Morphol 251:114–139.

Maisano JA. 2002b. Postnatal skeletal ontogeny in five xantusiids (Squamata: Scleroglossa) J Morphol 254:1–38.

Monteiro LR. 1998. Ontogenetic changes in the skull of *Corallus caninus* (L. 1758) and *Corallus enhydris* (L. 1758) (Serpentes-Boidae), an allometric study. The Snake 28:51–58.

Montero RC, Gans C, Lions ML. 1999. Embryonic development of the skeleton of *Amphisbaena darwini heterozonata* (Squamata: Amphisbaenidae). J Morphol 239:1–25.

Oelrich TM. 1956. The anatomy of the head of *Ctenosaura pectinata* (Iguanidae). Misc Pub Mus Zool Univ Michigan 94:1–122, 59 figures.

Olori JC, Bell CJ. 2012. Comparative skull morphology of uropeltid snakes (Alethinophidia: Uropeltidae) with special reference to disarticulated elements and variation. PLoS One 7:e32450.

Polachowski KM, Werneburg I. 2013. Late embryos and bony skull development in *Bothropoides jararaca* (Serpentes, Viperidae). Zoology 116:36–63.

Rieppel O. 1979. A cladistic classification of primitive snakes based on skull structure. Z Zool Syst Evolutionsforsch 17:140–150.

Rieppel O. 1980. The sound-transmiting apparatus in primitive snakes and its phylogenetic significance. Zoomorphology 96:45–62.

Rieppel O. 1984. Miniaturization of the lizard skull: its functional and evolutionary implications. In: Ferguson MWJ, editor. The structure, development and evolution of reptiles. London: The Zoological Society of London, Academic Press. p 503–520.

Rieppel O. 1988. A review of the origin of snakes. Evol Biol 22:37–130.

Rieppel O. 1989. The closure of the lateral braincase wall in snakes. Fortschr Zool 35:409–411.

Rieppel O. 1993. Patterns of diversity in the reptilian skull. In: Hanken J, Hall BK, editors. The skull, Vol. 2: Patterns of structural and systematic diversity. Chicago and London: University of Chicago Press. p 344–390.

Rieppel O. 2012. "Regressed" macrostomatan snakes. Fieldiana (Life and Earth Sci) 2012:99–103.

Rieppel O, Zaher H. 2001. The development of the skull in *Acrochordus granulatus* (Schneider) (Reptilia: Serpentes), with special consideration of the otico-occipital complex. J Morphol 249:252–266.

Rieppel O, Zaher H. 2002. The skull of the Uropeltinae (Reptilia, Serpentes), with special reference to the oticooccipital region. Bull Nat Hist Mus Zool Ser 68:123–130.

Rossman CE. 1980. Ontogenetic changes in skull proportions of the diamondback water snake, *Nerodia rhombifer*. Herpetologica 36: 42–46.

Scanferla A. 2010. The origin and evolution of snakes-Anatomical and phylogenetic analysis of Cretaceous and Paleogene ophidians from Patagonia and Bolivia. Ph.D. Dissertation. La Plata, Argentina: Universidad Nacional de La Plata. Available at http://sedici.unlp.edu.ar/handle/10915/4305

Scanlon JD. 2005. Cranial morphology of the Plio-Pleistocene giant madtsoiid snake *Wonambi naracoortensis*. Acta Palaeontol Pol 50: 139–180.

Scanlon JD. 2006. Skull of the large non-macrostomatan snake *Yurlunggur* from the Australian Oligo-Miocene. Nature 439:839–842.

Tarazona OA, Fabrezi M, Ramírez-Pinilla MP. 2008. Cranial morphology of *Bachia bicolor* (Squamata: Gymnophthalmidae) and its postnatal development. Zool J Linn Soc 152:775–792.

Tchernov E, Rieppel O, Zaher H, Polcyn MJ, Jacobs IJ. 2000. A new fossil snake with limbs. Science 287:2010–2012.

Torres-Carvajal O. 2003. Cranial osteology of the Andean lizard *Stenocercus guentheri* (Squamata: Tropiduridae) and its postembryonic development. J Morphol 255:94–113.

Wever EG. 1978. The reptile ear, its structure and function. NJ: Princeton University Press.

Wilson JA, Mohabey D, Peters S, Head JJ. 2010. Predation upon hatchling sauropod dinosaurs by a new basal snake from the Late Cretaceous of India. PLoS Biol 8:e1000322.

Young BA. 1989. Ontogenetic changes in the feeding system of the red-sided garter snake, *Thamnophis sirtalis parietalis*. J Zool 218:365–381.

Zaher H, Scanferla A. 2012. The skull of the Upper Cretaceous snake *Dinilysia patagonica* Smith-Woodward, 1901, and its phylogenetic position revisited. Zool J Linn Soc 164:194–238.

APPENDIX : SPECIMENS EXAMINED

Institutional Abbreviations

AMNH, American Museum of Natural History, New York; NHMUK, British Museum of Natural History, London; CAS, California Academy of Science, San Francisco; CENAI, Centro Nacional de Investigaciones Biológicas (currently housed in MACN), Buenos Aires; CM, Carnegie Museum of Natural History, Pittsburgh; FML, Fundación Miguel Lillo, Tucumán; FMNH, Field Museum of Natural History, Chicago; IB, Instituto Butantan, Sao Paulo; LSUMZ, Louisiana State University Museum of Zoology, Baton Rouge; MACN, Museo Argentino de Ciencias Naturales "Bernardino Rivadavia", Buenos Aires; MCN, Museo de Ciencias Naturales de Salta, Salta; MECN, Museo Ecuatoriano de Ciencias Naturales, Quito; MLP, Museo de La Plata, La Plata; MNHN, Museum National dÇHistoire Naturelle, Paris; MPEG, Museu Paraense "Emílio Goeldi", Belém; MUCPv, Museo Universidad Nacional del Comahue, Neuquén; MZUSP, Museu de Zoologia, Universidade de Sao Paulo, Sao Paulo.

Postnatal Sequence of *Dinilysia* patagonica

Playón de la Universidad del Comahue locality: MACN-N 106 and MUCPv 38; Boca del sapo locality: MLP 26–410 and MLP 71-VII-29-1; Paso Córdova locality: MACN-RN 976, MACN-RN 1013, MACN-RN 1014 and MPCA 527.

Comparative Postnatal Sequences

Liolaemus albiceps: MCN 2586 (subadult), MCN 2585 (adult)

Ophiodes intermedius: MCN 4443 (hatchling), MCN 4444 (adult)

Tupinambis merianae: MCN 4425 (subadult), MCN 4426 (adult)

Typhlops brongersmianus: MCN 4427 (juvenile), MCN 4428 (adult)

Epictia australis: MCN 4429 (juvenile), MCN 4430 (subadult), MCN 4431 (adult)

Anilius scytale: CENAI 3883 (subadult), IB 46686 (subadult), MZUSP 14574 (adult)

Python molurus: MCN 4433 (juvenile), MACN 39026 (adult)

Boa constrictor: MCN 4432 (juvenile), MACN 39025 (adult)

Hydrodynastes gigas: MLP JW-128 (juvenile), MLP JW-955 (subadult), MLP R-5143 (adult)

Liophis jaegueri: MCN 4434 (hatchling), MCN 4435 (adult)

Bothrops diporus: MCN 4436 (hatchling), MCN 4437 (subadult), MCN 4438 (adult)

Crotalus durissus: MCN 4439 (juvenile), MCN 4445 (adult)

Xenodon merremi: MCN 4440 (juvenile), MCN 4441 (subadult), 4442 (adult)

Adult Specimens

Achalinus formosanus (LSUMZ 19354; NHMUK 1983-192)*; Acrantophis madagascariensis* (MNHN 1983.484); *Acrantophis dumerili* (MZUSP 14430); *Acrochordus granulatus* (AMNH 66367); *Acrochordus javanicus* (AMNH 140813); *Ahaetulla ahaetulla* (MNHN C 952-36/-37/-38); *Ahaetulla prasina* (MNHN C 2943-29/-30/-31); *Ahaetulla subocularis* (MNHN 1973.142A); *Anilius scytale* (CENAI 3883, MACN 8817a, MACN 8817b, IB 46686, MZ 14572); *Antaresia childreni* (AMNH 86213); *Apostolepis dimidiata* (AMNH 62192); *Apostolepis flavotorquata* (AMNH 93559); *Aspidites melanocephala* (AMNH 18681); *Atractaspis irregularis* (MNHN 1991.4071/4072); *Bitis arietans* (CENAI 3386); *Boa constrictor* (MACN 39025, MZUSP 2553, MZUSP 13843); *Boiruna maculata* (MACN 40006, MACN 40007); *Boiruna sertaneja* (MZUSP 7031); *Bothrops alternatus* (MACN 40018); *Bungarus fasciatus* (CENAI 3887); *Calabaria reinhardtii* (AMNH 45901, CM 147738); *Candoia aspera* (AMNH 142843); *Candoia carinata* (MZ 14111, MZ 14112); *Casarea dussumieri* (MNHN 1992-27, MNHN 1993.3382); *Causus rhombeatus* (MNHN 1991.4146/4147); *Causus maculatus* (MNHN 1991.4140); *Causus resimus* (MNHN 1991.4144); *Cerberus rhynchops* (MNHN 1991.4352); *Charina bottae* (CM 36539, MZ, 8854); *Clelia rustica* (MACN 40004); *Corallus caninus* (CM 145320, IB 40869, MZUSP 14426); *Corallus hortulanus* (MZ 13050); *Cylindrophis maculatus* (AMNH 85496); *Cylindrophis ruffus* (AMNH 85647, CM 147774, MNHN 1970.411); *Daboia russelli* (MNHN 1991.4112/4113/4114, MNHN 1997.6005/6037); *Dasypeltis scabra* (CENAI 3853); *Dendroaspis polylepis* (MACN S/N); *Enhydris bocourti* (MNHN 1970-557A); *Enhydris enhydris* (MNHN C 3458-23/-24); *Enhydris innominata* (MNHN 1970-560A); *Enhydris plumbea* (MNHN C 3461-15/-19); *Enhydris dussumieri* (MNHN 2009.0206); *Enhydris jagorii* (MNHN 1970.554A); *Enhydris sieboldii* (MNHN 2009.0204); *Epicrates angulifer* (CM 35999); *Epicrates cenchria* (IB 52174, 49335); *Erpeton tentaculatus* (MNHN 1970.573A); *Eryx conicus* (AMNH 89273, CM 91863); *Eryx jaculus* (MZ 14101); *Eryx johni* (AMNH 99701); *Eryx miliaris* (AMNH 143770); *Eunectes murinus* (MPEG 16443); *Eunectes notaeus* (MZUSP 7622); *Eunectes deschauensis* (MPEG 18019); *Exiliboa placata* (AMNH 102892); *Helicops leopardinus* (MACN 40014); *Homalopsis buccata* (MNHN 1991.4202, MNHN 1991.4347, MNHN 1991.4348, MNHN 1970.519a); *Homoroselaps lacteus* (MNHN 1991.4162); *Hydrophis* sp. (MNHN 1986.0596); *Langaha nasuta* (MNHN 1991.4355, MNHN 1950.178A); *Leiopython albertisii* (AMNH 95140, MZUSP 14427); *Liasis fuscus* (AMNH 86222); *Lichanura roseofusca* (CM 56093, CM 145332, MZUSP 7283); *Ligophis anomalus* (MACN 40012); *Ligophis miliaris* (MACN 40013); *Ligophis poecilogyrus* (MACN 40011); *Loxocemus bicolor* (AMNH 110151, MZUSP 14114, FML 970, LSUMZ 49634); *Macrelaps microlepidotus* (CENAI 3858, LSUMZ 55387); *Madagascarophis colubrinus* (MNHN C 2451-37/-38); *Malpolon monsspesulanus* (MNHN 1988.6505, MNHN 1994.4175, MNHN 1991.4358, MNHN

1991.4562); *Mastigodryas bifossatus* (MACN 40017); *Mehelya capensis* (MACN 3857); *Mimophis madagascariensis* (MNHN 1989.2917, MNHN 1989.2918, MNHN 1989.2919, MNHN 1989.2961); *Morelia viridis* (AMNH 95135, MZUSP 14428); *Morelia spilota* (MNHN 1991.4048); *Naja nivea* (CENAI 3881); *Nerodia rhombifer* (CENAI 3838); *Notechis* sp. (MNHN 1991.4100); *Oxyrhabdium modestum* (LSUMZ 11814); *Oxyrhopus rhombifer* (MACN 40010); *Pareas mollendorfi* (AMNH 27770); *Parias sumatranus* (CENAI 3783); *Philodryas patagoniensis* (MACN 40008); *Philodryas mattogrossensis* (MACN 33420); *Philotamnus hoplogaster* (CENAI 3856); *Phimophis vittatus* (MACN 40005); *Psammophis crucifer* (MNHN 1991.4214); *Psammophis lineatus* (MNHN 1989.2942); *Psammophis sibilans* (MNHN 1991.4173, MNHN 1991.4565, MNHN 1991.4199/4200); *Pseudotyphlops philippinus* (BMNH 1978.1092); *Python molurus* (MACN 39026, MACN 39027); *Ramphiophis togoensis* (MNHN 1991.4184); *Ramphiophis maradiensis* (MNHN 1994.0587); *Rhinophis blythi* (AMNH 85076); *Rhinophis drummondhayi* (AMNH 85076); *Sanzinia madagascariensis* (MNHN 1900.122a); *Thamnodynastes hypoconia* (MACN 40016); *Trachyboa boulengeri* (MECN 2240, MZ 8247); *Trachyboa gularis* (AMNH 28982); *Tropidophis canus* (AMNH 73066, AMNH 45839); *Tropidophis feicki* (AMNH 81128, AMNH 81132); *Tropidophis melanurus* (AMNH 82880, AMNH 46690, AMNH 93002); *Tropidophis semicinctus* (AMNH 7386); *Tropidophis tackzanowskii* (MECN 3037); *Ungaliophis continentalis* (LSUMZ 55454); *Ungaliophis panamensis* (AMNH 58845, AMNH 62639); *Uropeltis ceylonicus* (AMNH 43343); *Uropeltis pulmeyensis* (MNHN 1994-756); *Uropeltis woodmansoni* (NHMUK 1930.5.8.73–74); *Vipera aspis* (MNHN 1991.4066, MNHN 1991.4107, MNHN 1982.169A); *Vipera ammodytes* (MNHN 1991.4068); *Vipera berus* (MNHN 1991.4128); *Vipera latasti* (MNHN 1991.4145); *Xenodon merremi* (MACN 40015); *Xenodon dorbignyi* (MACN 40009); *Xenopeltis unicolor* (MACN 7568, MZUSP 9665, MNHN 1991.4446, FMNH 11524); *Xylophis perroteti* (MNHN 1991.4426).

CT Scan Imagery

Comparative specimens available from the Digital Morphology Library at the University of Texas (www.digimorph.com)

Angolosaurus skoogi (juvenile) California Academy of Sciences (CAS 206977)

Angolosaurus skoogi (adult) California Academy of Sciences (CAS 206978)

Heloderma suspectum (juvenile) Texas Memorial Museum (TNHC 62767)

Heloderma suspectum (adult) Texas Memorial Museum (TNHC 62766)

Shinisaurus crocodylurus (juvenile) Texas Memorial Museum (TNHC 62987)

Shinisaurus crocodylurus (adult) Field Museum of Natural History (FMNH 215541)

Lampropeltis getula (late embryo) Texas Memorial Museum (uncatalogued)

Lampropeltis getula (adult) Field Museum of Natural History (FMNH 95184)